



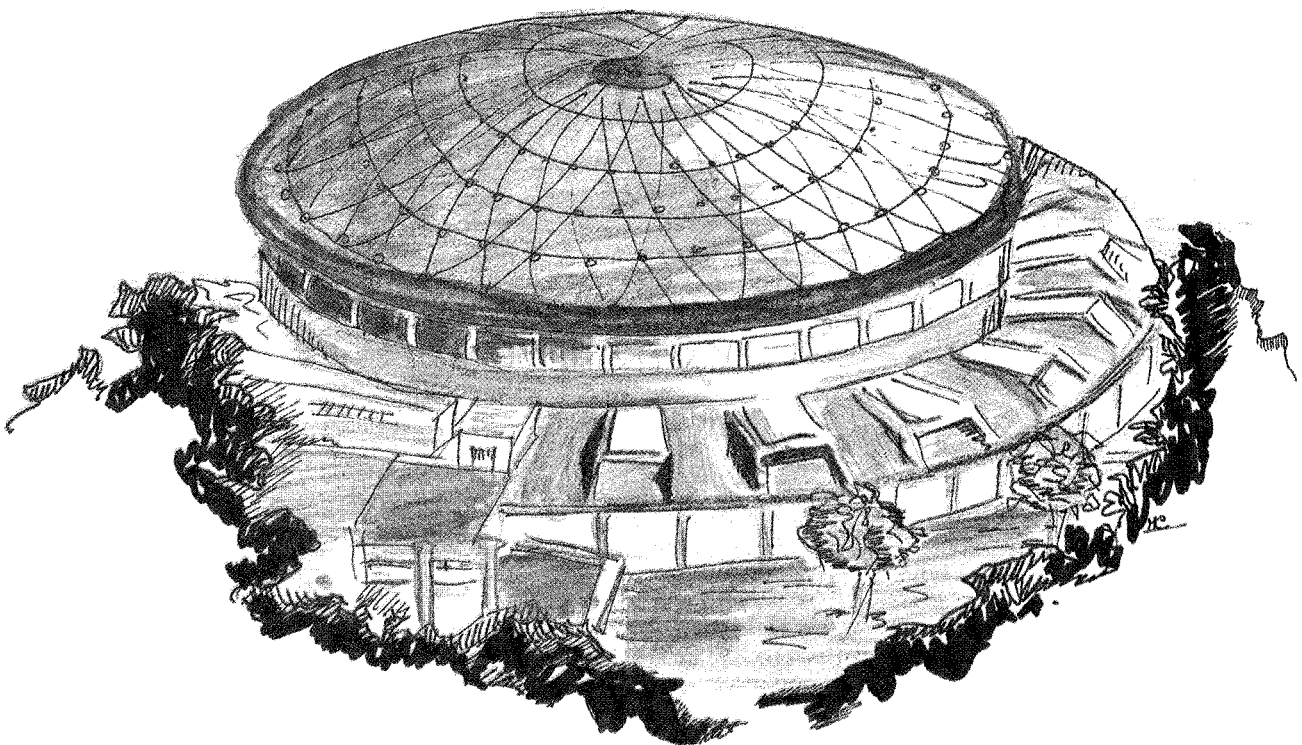
Laboratori Nazionali di Frascati

Submitted to Phys. Rev. B Rapid Commun.

LNF-88/42(PT)
7 Luglio 1988

M. Benfatto, C.R. Natoli, C. Brouder, R. F. Pettifer, M.F. Ruiz Lopez:

POLARIZED CURVED WAVE EXAFS: THEORY AND APPLICATION



Servizio Documentazione
dei Laboratori Nazionali di Frascati
P.O. Box, 13 - 00044 Frascati (Italy)

INFN - Laboratori Nazionali di Frascati
Servizio Documentazione

LNF-88/42(PT)
7 Luglio 1988

POLARIZED CURVED WAVE EXAFS: THEORY AND APPLICATION

M. Benfatto, C.R. Natoli,
INFN - Laboratori Nazionali di Frascati, P.O. Box 13, I-00044 Frascati, (Italy)

C. Brouder
Laboratoire de Physique du Solide, Université de Nancy I, B.P. 239, F-54506
Vandoeuvre-les-Nancy Cedex, (France)

R. F. Pettifer
Department of Physics, University of Warwick, Coventry, CV4 7AL, (England)

M.F. Ruiz Lopez
Laboratoire de Chimie Theorique, Université de Nancy I, B.P. 239, F-54506,
Vandoeuvre-les-Nancy Cedex, (France)

ABSTRACT

We derive, for the first time, an exact polarized extended x-ray absorption fine structure (EXAFS) formula valid for all edges which takes into account the curved wave nature of the electron propagators. We show that the deviations from the usual plane wave limit are not negligible and we discuss the physical implications concerning the determination of the Debye-Waller factors and coordination numbers. We apply our approach to recent surface extended x-ray absorption fine structure (SEXAFS) experiments regarding the study of the O(2x1)/Cu (110) system.

X-ray absorption spectroscopy (XAS) is a powerful technique for determining local atomic order in molecules and solids. One of the most important schemes for interpreting XAS spectra is the multiple scattering theory [1-2]. In this approach the absorption coefficient, under certain conditions, can be written as a series whose main term is the single scattering extended x-ray absorption fine structure (EXAFS) signal. This signal provides information on the pair distribution function [3]. The usual

approximation in EXAFS analysis is the so called plane wave (PW) approximation for the free electron propagators which enters into the expression of the EXAFS term [4]. Recently it has been shown that this approximation is always strictly invalid in the whole energy range of the XAS spectrum [5]. The appropriate approximation is not the PW, but rather an asymptotic form of the free electron propagators which includes spherical wave corrections and is simple enough to be suitable for calculations. This new approximation, called the spherical wave approximation (SW) [5], is in agreement with the exact calculation in the whole energy range of the XAS spectrum. This allows us to derive a simplified expression for the polarization-dependent EXAFS signal which includes spherical wave effects and is presented here for the first time both in its exact and approximate form. Moreover we discuss the physical implications of this new polarization-dependent EXAFS formula, in particular for what concerns the surface version of the EXAFS method of analysis, known as SEXAFS [6-7]. We also show the importance of the SW corrections in correctly determining the amplitude of the signal which is crucial when amplitude comparisons are made in order to obtain structural information such as coordination numbers, Debye-Waller factors etc. from experiments. In this context, in the last part of the paper, we compare some calculations based on our approach with recent experimental SEXAFS results regarding the study of the O(2x1)/Cu (110) system [8-9].

Before describing our approach it is useful to recall some results valid in the PW limit in order to see the most important differences. In particular we note that the polarization-dependent EXAFS term has the usual well known form (which we do not re-write here) with an effective coordination numbers given by (for K and L₁ edges) [10]:

$$N_i^* = \sum_{j=1}^{N_i} \cos^2 \theta_{ij}$$

for N_i atoms in the i-th shell. In this expression θ_{ij} is the angle between the electric field E and the internuclear bond axis. As a result, contributions coming from atoms whose bond axis is perpendicular to the electric field are exactly zero and no angular dependence is expected either in phase or in backscattering amplitude functions. This is not the case in the general treatment using curved wave as we shall see in a moment.

We now outline in some details our derivation. In the multiple scattering scheme the general expression for the absorption coefficient due to the excitation of a deep core level of angular momentum l_i can be written as [1-4] (L ≡ l, m):

$$\alpha_c = A \hbar \omega \frac{k}{\pi} \text{Im} \sum_{i, L, L', \sigma} (i | \vec{r} \cdot \vec{E} | R_i^0 Y_L \sigma) \tau_{LL'}^{00} (R_i^0 Y_L \sigma | \vec{r} \cdot \vec{E} | i) \quad (1)$$

where we have defined a scattering path (SP) operator given by [11]:

$$\tau_{LL'}^{00} = \frac{1}{\sin \delta_1} \frac{1}{\sin \delta_1} [(T_a^{-1} - G)^{-1}]_{LL'}^{00} = 1 + e^{i(\delta_1^0 + \delta_1'^0)} \sum_{n=0}^{\infty} [G (T_a G)^n]_{LL'}^{00}$$

In the above expression δ_1^i is the i -th phase shift of the atom located at site i and $T_a = \exp(i\delta_1^i) \sin(\delta_1^i) \delta_{ij}$, $\delta_{LL'}$ is the diagonal matrix made up of the individual atomic t_1 -matrices, $G_{LL'}^{ij}$ is the off-diagonal matrix in the site indices describing the free electron propagator between sites i and j (0 refers to the photoabsorbing site), R_1^0 is a function which behaves as $j_1 \cos \delta_1 - n_1 \sin \delta_1$ at the muffin-tin radius, k is the wave vector of the photoelectron and $A = 4\pi^2 \alpha n_c$, where α is the fine structure constant and n_c is the density of the excited atoms. The summation in Eq. (1) extends over all initial states i , partial outgoing and incoming waves $L L'$ and spin σ . The scattering path operator can be expanded in series when the spectral radius of the matrix $T_a G$ is less than one. In this way the multiple scattering (MS) series is generated. The EXAFS contribution is just the first ($n=1$) term in the MS series beyond the atomic one and involves single scattering only. The usual unpolarized expression is obtained by averaging over the directions of the electric field and using the PW limit for Hankel functions. In the following we do not adopt this scheme and provide corrections for wave curvature via a $g_{11'}^{(lm)}$ term; thus omitting for simplicity the site indices we use the relation

$$G_{LL'} = 4\pi Y_{10}^*(\hat{R}) Y_{10}(\hat{R}) \frac{e^{i\rho}}{\rho} g_{11'}^{(|m|)}(\rho) \delta_{mm'}$$

for the propagators which is valid when the z -axis is along the R direction⁵. We can use such a relation because in the single scattering approximation each atom acts independently so that its contribution to the EXAFS term has a cylindrical symmetry. In this expression $\rho = k \cdot R$ and Y_{1m} are spherical harmonics. A complete discussion concerning all the terms in the MS series, using a general form for the propagators, is given in Ref.12. The quantities $g_{11'}^{(lm)}$ in the propagator can be derived either exactly in term of Hankel functions by comparison with the expression for $G_{LL'}$ [1-4], or in an approximate way in terms of the leading factors of the modulus and phase asymptotic expansion of the Hankel functions. Both expressions will be given.

Using this expression for $G_{LL'}$, writing the scalar product $E \cdot r$ in term of the Legendre Polynomial P_1^m , keeping only the $n=1$ term in the MS series for the SP operator and summing over the spin orientations, after a little algebra, we obtain the wanted polarized curved wave EXAFS expression, written here for one scatterer:

$$\begin{aligned}
\alpha_2 = & A_0 \operatorname{Im} \left\{ \sum_{l,l'} I_{l,l'} I_{l,l'} (-1)^{l'} (2l_i + 1) (2l + 1) (2l' + 1) \begin{pmatrix} l_i & 1 & 1 \\ 0 & 0 & 0 \end{pmatrix} \begin{pmatrix} l' & 1 & l_i \\ 0 & 0 & 0 \end{pmatrix} \right. \\
& * \frac{e^{i(2\rho + \delta_l + \delta_{l'})}}{\rho^2} \sum_{m_\gamma, m, m_i} \begin{pmatrix} l_i & 1 & 1 \\ -m_i - m_\gamma & m & \end{pmatrix} \begin{pmatrix} l' & 1 & l_i \\ -m m_\gamma & m_i & \end{pmatrix} \frac{(1 - m_\gamma)!}{(1 + m_\gamma)!} \\
& * \left[P_1^{m_\gamma}(\cos \theta) \right]^2 \sum_{\lambda} (-1)^\lambda (2\lambda + 1) t_\lambda g_{1\lambda}^{|\lambda|}(\rho) g_{1'\lambda}^{|\lambda|}(\rho) \left. \right\} \quad (2)
\end{aligned}$$

where θ is the angle between the electric field E and the bond direction and $m_\lambda = 0, \pm 1$ is the azimuthal quantum number of the photon. In this expression the 3-j symbols gives the usual constraints on the angular momenta and the quantities $I_{l,l'}$ are the dipole radial integrals between the radial wave function of the initial core state of angular momentum l_i and the scattering solution R_l^0 calculated at the photoabsorbing site 0. The quantity A_0 is given by $A_0 = 2 A \hbar \omega k/\pi$.

For K or L_1 edge ($l_i = 0, m_i = 0, l = l'$) it is possible to simplify the EXAFS expression further to obtain:

$$\alpha_2 = -A_0 |I_{01}|^2 \operatorname{Im} \left\{ \frac{e^{2i(\delta_1 + \rho)}}{\rho^2} \sum_l (-1)^l (2l + 1) t_l [\cos^2 \theta (g_{11}^{(0)}(\rho))^2 + \sin^2 \theta (g_{11}^{(1)}(\rho))^2] \right\} \quad (3)$$

where

$$g_{11}^{(0)}(\rho) = \frac{(1+1)C_{1+1}(\rho) + 1C_{1-1}(\rho)}{2l+1} \quad (3a)$$

$$g_{11}^{(1)}(\rho) = \left[\frac{1(1+1)}{2} \right]^{\frac{1}{2}} \frac{C_{1+1}(\rho) - C_{1-1}(\rho)}{2l+1} \quad (3b)$$

The quantities C_l can be written as:

$$C_l(\rho) = i^{(1+1)} \rho e^{-i\rho} h_1^+(\rho) \approx \left[1 + \frac{1(1+1)}{2\rho^2} \right]^{\frac{1}{2}} e^{i\frac{1(1+1)}{2\rho}} \quad (3c)$$

The last expression is the SW approximation. Note that when $\rho \rightarrow \infty$ the quantities $g_{11}^{(0)} \rightarrow 1$ and $g_{11}^{(1)} \rightarrow 0$ recovering the usual plane wave limit. Moreover averaging over the field polarizations we obtain Rehr et al. result⁵. The importance of Eq. (3) lies in the presence of a new term proportional to the $\sin^2\theta$. This fact has two main implications: firstly, the phase and amplitude functions in EXAFS signal are now angle dependent and secondly there are contributions from atoms perpendicular to the electric field. Alternatively we can state that we find the usual $\cos^2\theta$ dependence plus an unusual anisotropic component. To evaluate the importance of this new term we plot the quantity RG versus $k \cdot R$ in Fig. 1 where RG is the modulus of the ratio between the square of the functions $g_{11}^{(1)}$ and $g_{11}^{(0)}$ calculated for various l values ranging from $l=1$ to $l=6$, (this ratio is always 0 for the $l=0$). This quantity which does not depend on the physical system, gives the strength of the $\sin^2\theta$ term versus the $\cos^2\theta$ term. This ratio is substantially different from zero for a wide range of values of the product $k \cdot R$ and becomes negligible only for values of order $18+20$ (for high l 's). Therefore we expect deviations from the PW behaviour in a large energy range of the XAS spectrum. It is interesting to note that as the interatomic distance R decreases the range of k values for which this effect becomes appreciable increases. Further intuition concerning the origin of the $\sin^2\theta$ term can be obtained by noting that if the radius of the atomic scattering potential collapses to a point then only s-wave scattering ($L=0$) is possible, and the $\sin^2\theta$ term disappears. Consequently the $\sin^2\theta$ term is associated with high L components whose magnitude at a given energy, related to t_l , reflects the size of the scattering. We should thus expect that the corrections will depend upon the atomic number Z of the scatterer.

Also, at low photoelectron energies where only a few phase shifts dominate the scattering we anticipate oscillations in the magnitude of the $\sin^2\theta$ contribution.

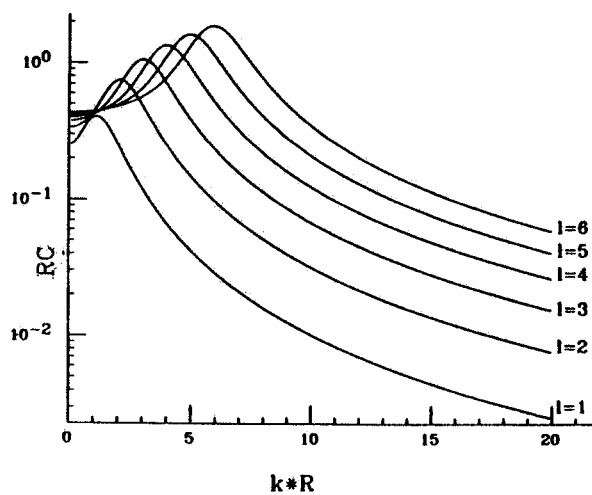


FIG. 1 - The RG function (see the text for definition) versus $K \cdot R$ and for various l value.

A classical analogue of the effect of the $\sin^2\theta$ term which dominates at $\theta=\pi/2$ can be envisaged. We consider a dipole radiation (analogue of the absorbing atom under K-shell excitation) with a scattering object (analogue of the scattering atom) positioned at a node in the radiation pattern. As the angle subtended by the object at the dipole increases the object itself is capable of intercepting and scattering progressively larger amounts of the radiation from the dipole. The angle subtended is a function of distance of the scattering object from the emitter, energy via the change of the back-scattering cross-section, and size of the scattering object.

The physical effects of the these SW corrections becomes clearer in Fig. 2. where the amplitude ratio A_2/A_1 of two EXAFS signals, calculated using Eq. (3), for two different angles θ is depicted. In the same Figure the PW limit is also shown as a dotted line.

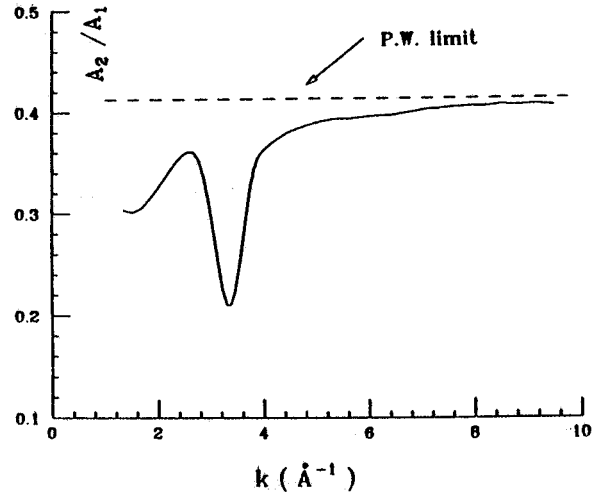


FIG. 2 - Amplitude EXAFS ratio versus k referred to the theoretical experiment described in the text. The full line is calculated by Eq. (3).

This calculation refers to the O K-edge absorption of an ideal cluster composed of an oxygen atom and a Cu scatterer ($Z=29$) located at a distance of 1.82 \AA . A_1 is for $\theta_1 = 0^\circ$ while A_2 is for $\theta_2 = 50^\circ$. The deviation from the plane wave behaviour is clear and important in a wide range of k values and only for $k \geq 8 \text{ \AA}^{-1}$ the difference between the PW and the SW regime becomes negligible. The important point is that contrary to the PW case the ratio A_2/A_1 now depends strongly on the energy. From this discussion it follows that the SW corrections to the "standard" EXAFS formula should be included in the analysis in order to determine correctly the coordination numbers and the Debye-Waller factors. Moreover these corrections are important for the selection of different structural models by amplitude comparison. It has recently been shown that the usual exponential form of the Debye-Waller factor in the EXAFS formula valid for a Gaussian pair correlation function can also be adopted when curved wave electron propagators are used^{13,14} because the phase and amplitude corrections due to this type of propagators are in fact negligible. Consequently we are now able to propose the following expression for the polarized curved wave EXAFS signal (written for simplicity just for the K and L_1 edges):

$$\alpha_2 = -A_0 |I_{01}|^2 \text{Im} \sum_{i=1}^{N_i} \sum_{j=1}^{N_j} \left\{ \frac{e^{2i(\delta_1 + \rho_i)}}{\rho_i} e^{-\frac{2R_i}{\lambda_{ij}}} \sum_1 (-1)^l (2l+1) t_1^i \right. \\ \left. * [\cos^2 \theta_{ij} [g_{11}^{(0)}(kR_i)]^2 + \sin^2 \theta_{ij} [g_{11}^{(1)}(kR_i)]^2] e^{-2k^2 \sigma_{ij}^2} \right\} \quad (4)$$

where N_i is the number of atoms in the i -th shell, θ_{ij} is the angle between the electric field E and bond axis R_i and σ_{ij} is the usual mean square relative displacement. We have also included the exponential decay factor due to the inelastic losses and possible anisotropies in Debye-Waller and mean-free path factors^{9,15,16}.

As an application we have simulated recent SEXAFS signals for chemisorbed oxygen on Cu (110). We refer to the paper of M. Bader et al. for notations and experimental details. In this paper the

authors employ the conventional procedure based on the amplitude ratio comparison to study different structural surface models and to derive Debye-Waller and mean-free path factors. In particular, using the Fourier and Back-Fourier procedure, they find the behaviour of the EXAFS amplitude ratio as a function of k^2 for various azimuthal and polar angles. In the following we concentrate our attention on the case $A_2(45^\circ)/A_1(90^\circ)$. The angles given in parentheses are the polar angles while the amplitudes A_1 and A_2 have been measured in the azimuth $[001]$ and $[1\bar{1}0]$ respectively. Due to the fact that the experimental amplitude ratios can not be fitted by any surface reconstruction model they predict an anisotropy in the mean free path factors. Our objection is that the experimental values are compared with theoretical predictions made by the PW limit of the theory. For example, for this case the experimental value is 0.31 at $k=4\text{\AA}^{-1}$ while the theoretical value, calculated using the missing row model and the plane wave theory of EXAFS, is about 0.38 taking $\Delta\sigma^2 = 2.4 \cdot 10^{-3} \text{\AA}^2$ for the Debye-Waller anisotropy and $\lambda = 5.2 \text{\AA}$ for the mean-free path value. The situation changes if the SW corrections are included. In Fig. 3 we report the quantity $\ln[A_2(45^\circ)/A_1(90^\circ)]$ as a function of the photoelectron wave number k calculated with the same choice of the Debye-Waller anisotropy and mean free path value and using the missing row reconstruction model for the structure. The continuous line is calculated using Eq. 4. For comparison the PW limit of the theory is also shown as a dashed-dots line. In order to make contact with the procedure used to extract experimental data (reported in Fig. 3 as points with errors bars) we have used the conventional Fourier Transform (FT) method to compute theoretical amplitudes $A_2(45^\circ)$ and $A_1(90^\circ)$. More precisely, we have first calculated the FT of the EXAFS theoretical signal for the two cases in a wave vector range going from 1 to 10\AA^{-1} . Secondly, the back-transform of the Fourier peaks has been taken, using a window from 0.9 to 2.75\AA , to give the required amplitudes. Then the logarithm of the amplitude ratio $A_2(45^\circ)/A_1(90^\circ)$ has been computed and plotted as a dashed line in Fig. 3. This method yields results which are in reasonable agreement with the exact calculation given by Eq. 4. Nevertheless this method depends strongly on the choice of the back Fourier window as we have verified. In any case the agreement between theory and experimental data is now definitely better than when the PW approximation is used. The remaining discrepancies can be assigned either to some anisotropies in the mean free path value, which have not been included in our calculation, or to the treatment of the experimental data in terms of Fourier and Back Fourier procedure.

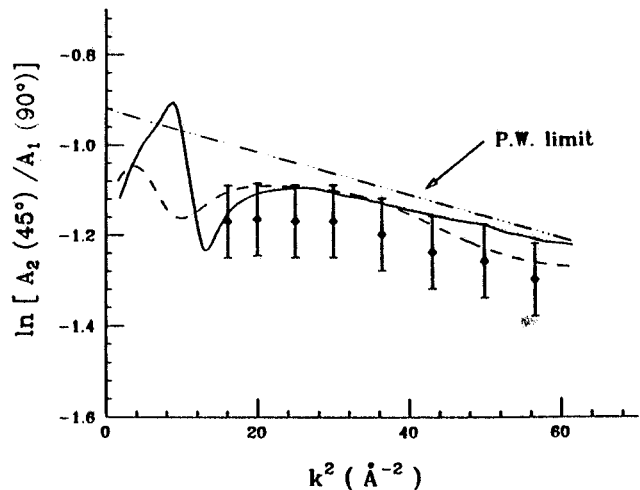


FIG. 3 - Comparison between experimental value of logarithm of SEXAFS amplitude ratio as a function of k^2 (points with errors bars) with various theoretical calculations. The full line is referred to Eq. (4) of the text, the dashed line to the Fourier Back-Fourier treatment of the SW theoretical calculation while the dash-dotted line is the PW limit of the theory.

In conclusion we have derived, for the first time, a polarized EXAFS formula which accounts quite well for the curved nature of the free electron propagators and at the same time is easy to compute. Moreover we have shown that the resulting corrections are important in a relevant energy range of the spectrum (up to 150+200 eV above the edge) and should be included to reproduce quantitatively the experimental results in order to discriminate between different structural models and obtain reliable numbers for the " amplitude factors " as coordination, Debye-Waller and mean-free path values. Thirdly, we have reconfirmed the missing row reconstruction model for the O(2x1)/Cu(110) system in agreement with M. Bader et al. without having to invoke any anisotropy in the mean free path values.

We want to thank Dr. L. Incoccia for the critical comments and Dr. E. Pace for computing help.

REFERENCES

- 1) C.R. Natoli and M. Benfatto, in " EXAFS and NEAR EDGE STRUCTURE IV " edited by P. Lagarde, D. Raoux and J. Petiau, J. Phys (Paris) Colloq. **47**, C8-11 (1986); P. J. Durham, J.B. Pendry and C.H. Hodges, Comput. Phys. Commun. **25**, 193 (1982).
- 2) For reviews, see E.A. Stern and S.M. Heald in " HANDBOOK of SYNCHROTRON RADIATION" edited by E.E. Kock (North-Holland, New York 1983) chap. 10; "EXAFS and NEAR EDGE STRUCTURE" vol. 27 of Springer Series in Chemical Physics edited by A. Bianconi, L. Incoccia and S. Stipcich (Springer Verlag, Berlin 1983).
- 3) D.E. Sayers, E.A. Stern and F.W. Lytle, Phys. Rev. Lett. **27**, 1204 (1971).
- 4) W.L. Schaich, Phys. Rev. B **29**, 6513 (1984).
- 5) J.J. Rehr, R.C. Albers, C.R. Natoli and E.A. Stern, Phys. Rev. **B34**, 4350 (1986).
- (6) P.H. Citrin, P. Eisenberger and R.C. Hewitt, Phys. Rev. Lett. **41**, 309 (1978).
- (7) P.H. Citrin, P. Eisenberger and J.E. Rowe, Phys. Rev. Lett. **48**, 802 (1982).
- (8) U. Dobler, K. Baberschke, J. Hoose and A. Puschmann, Phys. Rev. Lett. **52**, 1437 (1984).
- (9) M. Bader, A. Puschmann, C. Ocal and J. Hoose, Phys. Rev. Lett. **57**, 3273 (1986).
- (10) For a review we refer the reader to J. Stohr, in " PRINCIPLES, TECHNIQUES and APPLICATION of EXAFS, SEXAFS and XANES" edited by D. Koningsberger and R. Prinz (Wiley, New York 1984).
- (11) M. Benfatto, C.R. Natoli, A. Bianconi, J. Garcia, A. Marcelli, M. Fanfoni and I. Davoli, Phys. Rev. **B34**, 5774 (1986).
- (12) C. Brouder, M.F. Ruiz-Lopez, R.F. Pettifer, M. Benfatto and C.R. Natoli submitted Phys. Rev. B (1988).
- (13) M. Benfatto, C.R. Natoli, and A. Filipponi, submitted to Phys. Rev. B (1988).
- (14) C. Brouder, Submitted to Phys. Rev. B (1988).
- (15) R. Roubin, D. Chandrossis, G. Rossi, J. Lecante, M.C. Desjournes and G. Treglia, Phys. Rev. Lett. **56**, 1272 (1986).
- (16) F. Sette, C.T. Chen, J.E. Rowe and P.H. Citrin, Phys. Rev. Lett. **59**, 311 (1987).